

## Removal of $\text{Cd}^{2+}$ , $\text{As}^{3+}$ , $\text{Cr}^{2+}$ , $\text{Ni}^{2+}$ and $\text{Pb}^{2+}$ ions From Industrial Wastewater Using MnO and Modified MnO Nanoparticles

<sup>1</sup>Igwe, P. U., <sup>2</sup>Oguzie, E. E., <sup>1</sup>Uzoije, A., P., and <sup>1</sup>Ebe, T. E.

<sup>1</sup>Department of Environmental Management, Faculty of Environmental Sciences,  
Federal University of Technology, Owerri

<sup>2</sup>Department of Chemistry, Faculty of Science, Federal University of Technology, Owerri  
DOI: 10.56201/ijccp.v10.no6.2024.pg75.86

### Abstract

Manganese oxide as a nano-adsorbent was synthesized and characterised by X-ray diffraction (XRD) Scanning electron microscope (SEM), Infrared Spectroscopy (FT-IR) and X-ray Fluorescence (X-RF). The adsorption of  $\text{Cd}^{2+}$ ,  $\text{As}^{3+}$ ,  $\text{Cr}^{2+}$ ,  $\text{Ni}^{2+}$  and  $\text{Pb}^{2+}$  ions from aqueous solution on the manganese oxide were investigated with variation in contact time, initial concentration of metal ions in solution and adsorbent mass. The results showed that the adsorption of the metal ions increased at 25mins and reached equilibrium gradually and removal percentages were 83%, 57%, 42% and 38% for 10ppm, 20ppm, 30ppm, 40ppm and 50ppm respectively by using 0.5g/mols for 60mins at pH of 4. The results also revealed that both the coated and noncoated were a promising adsorbent for the removal of  $\text{Cd}^{2+}$ ,  $\text{As}^{3+}$ ,  $\text{Ni}^{2+}$ ,  $\text{Cr}^{6+}$  and  $\text{Pb}^{2+}$  ions from wastewater.

**Keywords:** Adsorption, heavy metals, manganese oxide, nanoparticles, starch, wastewater

### INTRODUCTION

Though water has an important part used for the processes of different manufacturing or mining activities, still the wastewater that is released into the environment during the process is associated with contaminants. The treatment of the discharged effluents or wastewater from these processes has not been given the required attention. The producers and the consumers of products from industrial processes are only concerned with the quality of the product without proper understanding or expertise in wastewater treatment. In addition to the non-concern of wastewater treatment by end-users, it is vital for dropping the hazard in the manufacturing processes (Chen, et al., 2010). Nevertheless, the management and controlling of water in production has turned out to be more extremely accepted in the past few years as a notable subject in line for the growing pressure on water resorts and low value feed water, because fresh water is becoming increasingly challenging to be found (Qu et al., 2013; Teh et al., 2014).

Accordingly, industrial products manufacturers are doubling their efforts to reduce the wastewater influence on freshwater resources. This is achieved through the method of treatment of used water before discharge into the environment. Excess of wastewater and absence of clean water drives government and residents to spend more on drinkable water and its rational applications. Water treatment expertise has helped to decrease and totally remove the detrimental effect on the environs, and assist in the maintenance of equilibrium in natural water systems (Isidorov, 1997). The existence of heavy metals in wastewater has been largely due to increase in the growth of industry and human activities, such as, petrochemicals, plating and electroplating industry, rayon industry, batteries, paper manufacturing, pesticides, metal rinse processes, tanning industry, textile

industry, metal smelting, mining industry, fluidized bed bioreactors, and electrolysis applications. The wastewater contaminated with heavy metals finds its way into the environment, thereby threatening human health and the general ecosystem. Heavy metals are known to be non-biodegradable and in most instances have been reported to be carcinogenic (El-Sherif et al., 2013; García-Niño & Pedraza-Chaverrí, 2014; Taseidifar et al., 2017), hence, the occurrence of these heavy metals in water in large amounts or quantities could bring about critical health concerns to humans and other living organisms.

Poisonous heavy metal contamination is very important in environmental and occupational considerations due to the propensity of heavy metals to be integrated into the food chain (Sikder *et al.*, 2014). Numerous conservative methods such as chemical precipitation, filtration, chemical oxidation or reduction, electrochemical treatment, reverse osmosis, ion exchange and evaporation have been used to remove heavy metals from weak solutions (Das, 2015). Although, these methods regularly are associated with the problem of not being able to remove contaminants to acceptable discharge limits. The main issue connected with these methods involve very high operational cost and the production of other chemicals as by-products, which also might constitute environmental hazard (Wang & Chen, 2014). So, there is a need to search for a cost effective and eco- friendly alternative technique for removal of heavy metals from aqueous environment. The contamination of aquatic environment is one of the most serious worldwide human health threat due to its extremely toxic effects on animals and plants. Various treatment technologies such as coagulation and precipitation, adsorption, membrane filtration, ion exchange, reverse osmosis and phytoremediation, have been developed for the removal of toxic metals and other deleterious components or chemicals from drinking water and wastewater.

The most common heavy metals often found in wastewater are lead (Pb), copper (Cu), nickel (Ni), arsenic (As), cadmium (Cd), zinc (Zn), chromium (Cr), and mercury (Hg). Even though these heavy metals can be identified in trace quantities; nevertheless, they are still harmful. The above-mentioned heavy metals and others like iron (Fe), silver (Ag), manganese (Mn), cobalt (Co), molybdenum (Mo), calcium (Ca), boron (B), antimony (Sb), etc. are usually obtainable in wastewater and therefore the need to be removed (Qasem et al., 2021).

Sources of water pollution are natural and man-made sources. Hence, the type of treatment suitable for wastewater becomes a very important issue that is associated with the types of wastewaters generated. Generally, wastewater is classified since the domination of either organic based compounds or inorganic material it contains. The presence of toxic metals in the environment play a very negative role which is very unsafe for the environment and can cause death for man and animals. Manufacturing and prospecting industries are the most notable sources of anthropogenic poisonous metals. Generally, anthropogenic input sources of toxic heavy metals include the fuel industry, machinery, traffic, ferrous metallurgy, non-ferrous metallurgy, mining industry, chemical industry, electroplating.

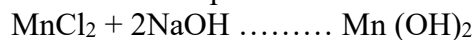
### **Materials and methods**

All chemicals used were of analytical grade Hydrated manganese Chloride [ $\text{MnCl}_2 \cdot 4\text{H}_2\text{O}$ ] with Sodium Hydroxide [NaOH]

#### **Preparation of the Nano-adsorbent**

The method of Konne and Opara (2014) was used in the preparation of MnO adsorbent. 13.21grams of  $\text{MnCl}_2$  was dissolved in deionized water and was reacted in 20.0grams of NaOH at

1:1 ratio. The Mn (OH)<sub>2</sub> was filtered and dried until a golden yellow precipitate appeared. It was dried at 80C to produce a dark brownish crystal of MnO.



The manganese with starch were dissolved 0.2grams of dried starch powder in 100ml of de-aerated water. The manganese (II) Oxide (MnO) nanoparticle was synthesized by a wet chemical method. 13.21 grams of MnCl<sub>2</sub> dissolved in deionized water and was reacted in 20.0grams of NaOH at 1:1 ratio. The Mn (OH)<sub>2</sub> was filtered and dried until a golden yellow precipitate appeared. It was dried at 80C to produce a dark brownish crystal of MnO.



### The Column experiment

A stock solution of cadmium, nickel arsenic, chromium and lead were prepared by dissolving 1.348, 1.63, 2.21, 3.73 and 4.16 grams respectively of analytical reagent grade of each in de-ionized and 10ml of concentrated sulphuric acid and diluted to 1litre with de-ionized distilled water. Equilibrium isotherm for Cd<sup>2+</sup>, Ni<sup>2+</sup> and Pb<sup>2+</sup> ions were obtained by performing column adsorption studies.

### Preparation and characterization of MnO-SS nanoparticles.

Scanning Electron Microscopy (SEM) characterization was performed to identify surface morphology and size distribution of MnO-SS nanoparticles. The functional groups presenting in the MnO-SS nanoparticles was investigated using the Fourier transform infrared (FTIR) technique. X-ray diffraction (XRD) analysis was performed to identify the structure and composition of freshly synthesized MnO-SS nanoparticles.

### Adsorption experiments

Laboratory column experiments were carried out to study the adsorption of some heavy metals (As, Cd, Cr, Ni and Pb) on MnO-SS nanoparticles. The experiments were performed at room temperature (30°C) using 250 ml Erlen Mayer containing 50 mL solution of the heavy metals. The heavy metals solution was prepared by dissolving each in 0.1 M KNO<sub>3</sub> solution. A known amount of MnO-SS nanoparticles was added to 50 mL of corresponding heavy metal solution over a period. After the aqueous phase was separated, the concentration of heavy metal under consideration in the solution was determined by using an atomic absorption spectrometer.

The adsorption of each heavy metal by MnO-SS nanoparticles was investigated at pH range of 3-9. The initial pH of solution was adjusted by using 0.1 M HCl or 0.1 M NaOH. The effect of contact time (10, 20, 30, 40 and 50 mins.), initial concentration of the metals (10, 20, 30, 40 and 50 ppm) and amount of adsorbent dosage (0.1, 0.2, 0.3, 0.4 and 0.5 g) were also examined throughout the experiments at (30 °C). The amount of metal removal was calculated from the difference between metal taken and that remained in the adsorbent. The removal efficiency (R) of cadmium was calculated as:

$$R = \frac{C_i - C_f}{C_i} * 100 \quad (1)$$

The amount of metal adsorbed on the sorbent phase (mg g<sup>-1</sup>) was calculated as:

$$q = \frac{C_i - C_f}{m} * V \quad (2)$$

Where q is the amount of heavy metal adsorbed per unit weight of adsorbent, V is the volume of the liquid phase ( L), m is the weight of the adsorbent (g) and C<sub>i</sub> and C<sub>f</sub> are the initial and final concentrations of metal ion (mg L<sup>-1</sup>) in water.

### Results and discussion

### Characterization of adsorbent.

The results of X-Ray Diffraction Analysis of MnO+SS and MnO were shown in Figure 4.2. The XRD pattern as indexed with PC-APD diffraction software is a plot of intensity against 2-theta. The XRD patterns showed sharper peaks with fewer impurities for the MnO+S compared to that of the control MnO. However, there were more MnO peaks in the MnO+S patterns than in the control. This implied that the presence of starch allowed for the formation of more of the dioxide impurity phases. Starch also supported the formation of larger particle sized MnO+S nanoparticles. The estimated particle sizes of the MnO indexed peaks gave 51.984 and 34.083nm for the MnO+S and MnO respectively. The MnO showed more affinity for starch. This agreed with the broader peaks pattern observed in the MnO compared to the MnO+S broad peaks.

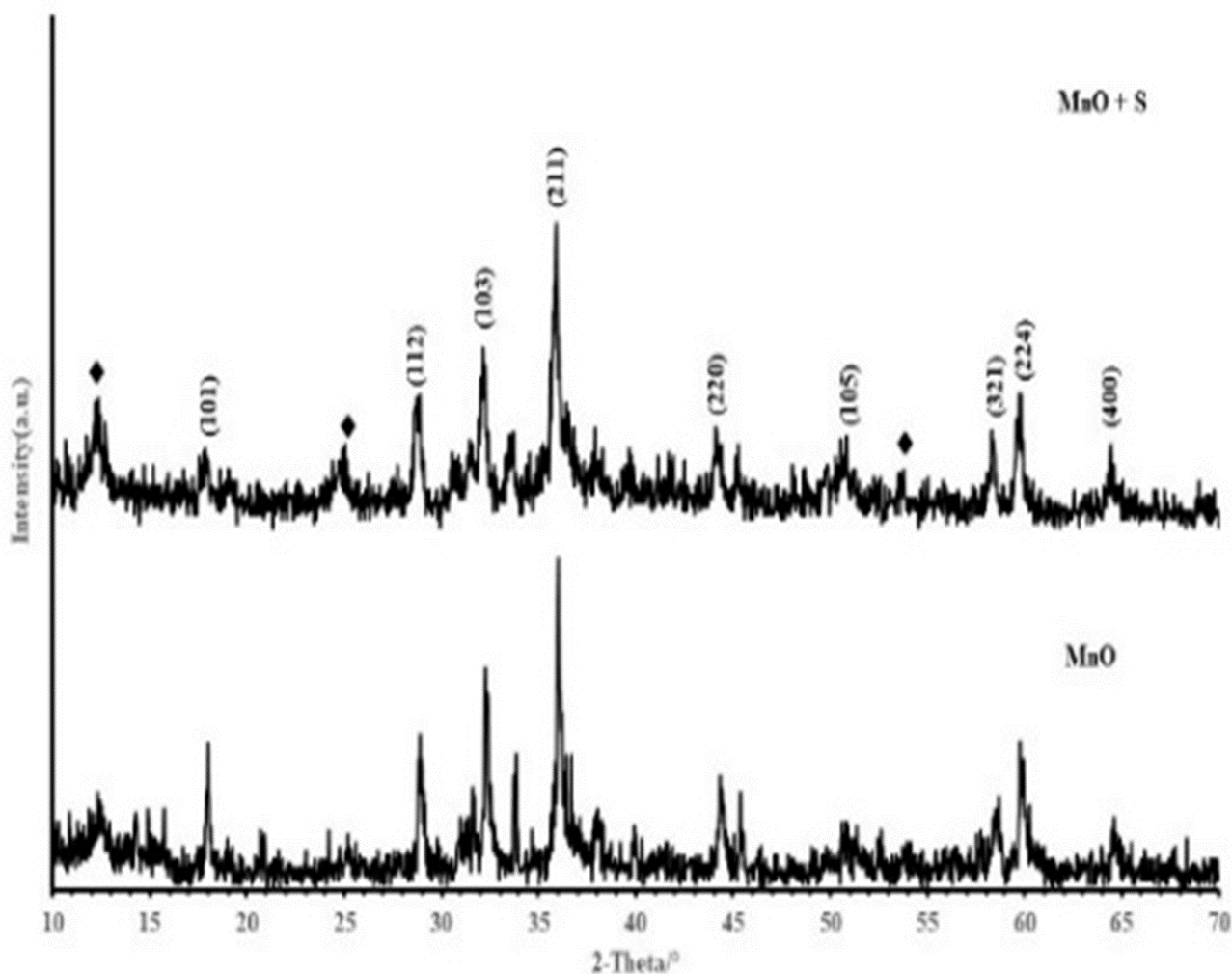


**Figure 1: The XRD of manganese oxide (MnO)**

The surface of the control sample (MnO) revealed a rough, porous plate-like polycrystalline, while that of the sample with (MnO-SS) appeared as platy but with more organized net-like pores.

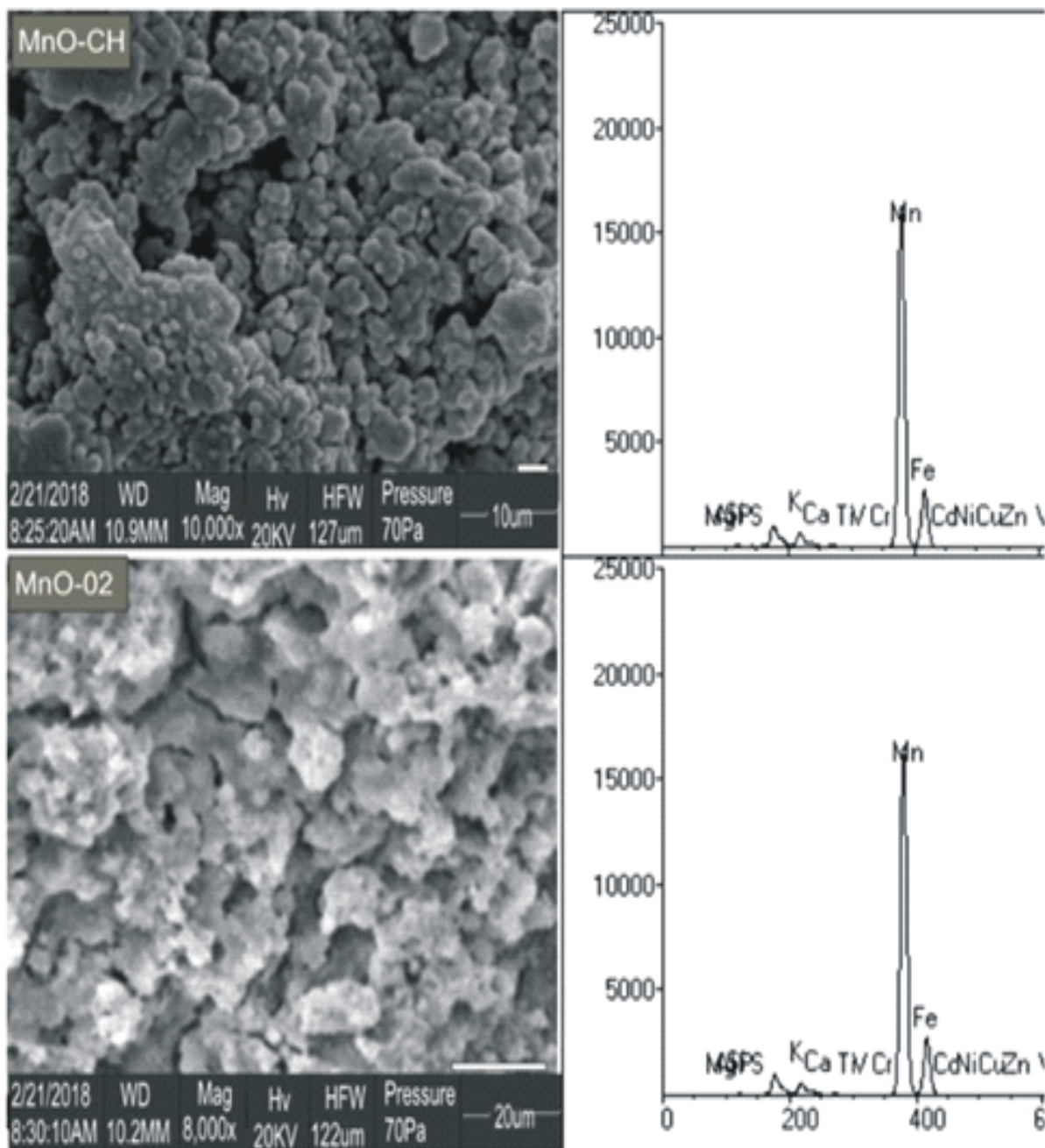


Plate 1: The details of surface morphology of the synthesized MnO+SS and MnO obtained from scanning electron microscopy (a/b) with their energy dispersive spectroscopy (EDS) C/D respectively.

The synthesized MnO were characterized using FTIR and the analysis was shown in Figures 4.8 (a and b). It was observed that the MnO with starch showed bands at 480.84, 497.20 and 513.79  $\text{cm}^{-1}$  which indicated the vibration of the metal-Oxygen bond (Mn-O). Absorption peaks observed at 2967.49 and 2924.00  $\text{cm}^{-1}$  were due to  $-\text{CH}_3$  stretching vibrations. The absorption peaks at 2471.7, 2374.34, 2341.18, 1449.74 and 1409.5 may be due to  $-\text{CH}_2$  stretching,  $=\text{C}-\text{H}$  stretching and  $-\text{C}-\text{H}$  stretching vibrations. For MnO without starch, the following bands waves observed at 518.20, 687.36, 898.89 and 977.7  $\text{cm}^{-1}$  indicating the vibration of the Mn-Oxygen bond (Mn-O). Absorption peaks observed at 2992.6 may be due to  $-\text{CH}_3$  stretching vibrations. The absorption peaks at 2896.6, 2468.3, 2345.57, 1812.81, 1628.99, 1449.49 and 1384.70  $\text{cm}^{-1}$  may be due to  $-\text{CH}_2$  stretching,  $=\text{C}-\text{H}$  stretching and  $-\text{C}-\text{H}$  stretching vibrations.

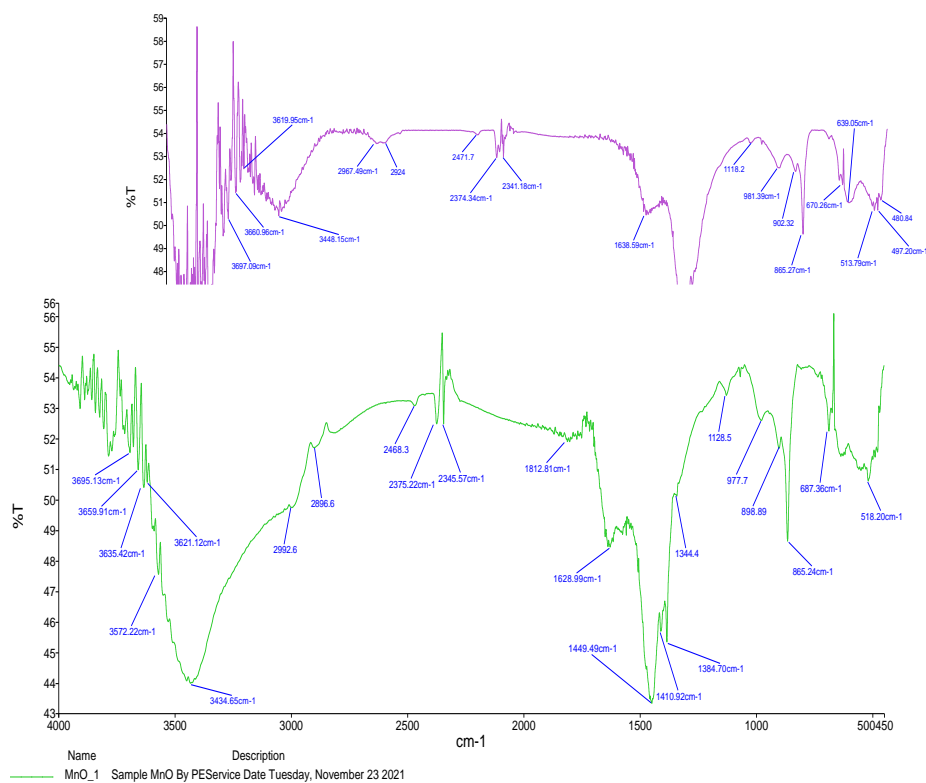


Figure 2: The FT-IR spectra of the Manganese Oxide (MnO) nanoparticles synthesised with and without starch respectively (a, b) in wave number range  $450-4000\text{cm}^{-1}$

### The effect of contact time

The effects of varying contact time of adsorption resulting to various degrees of % removal of  $\text{As}^{3+}$ ,  $\text{Cd}^{2+}$ ,  $\text{Cr}^{6+}$ ,  $\text{Ni}^{2+}$  and  $\text{Pb}^{2+}$  ions were carried out at time intervals of 5, 10, 15, 20 and 25 minutes and at constant adsorbent mass of 0.5grams, solution concentration of 50mg/l and temperature of  $40^\circ\text{C}$ . The effects of contact time in adsorption process of metal ion contaminants on MnO and MnO-SS are shown in the figure below.

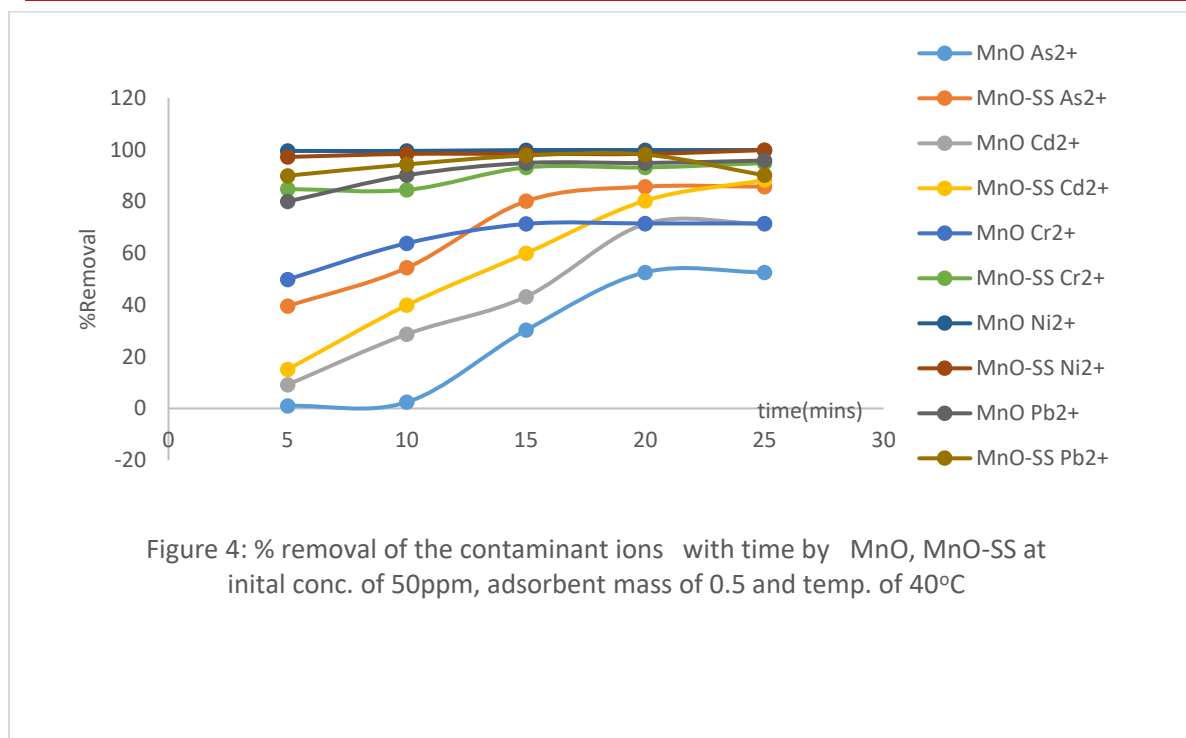


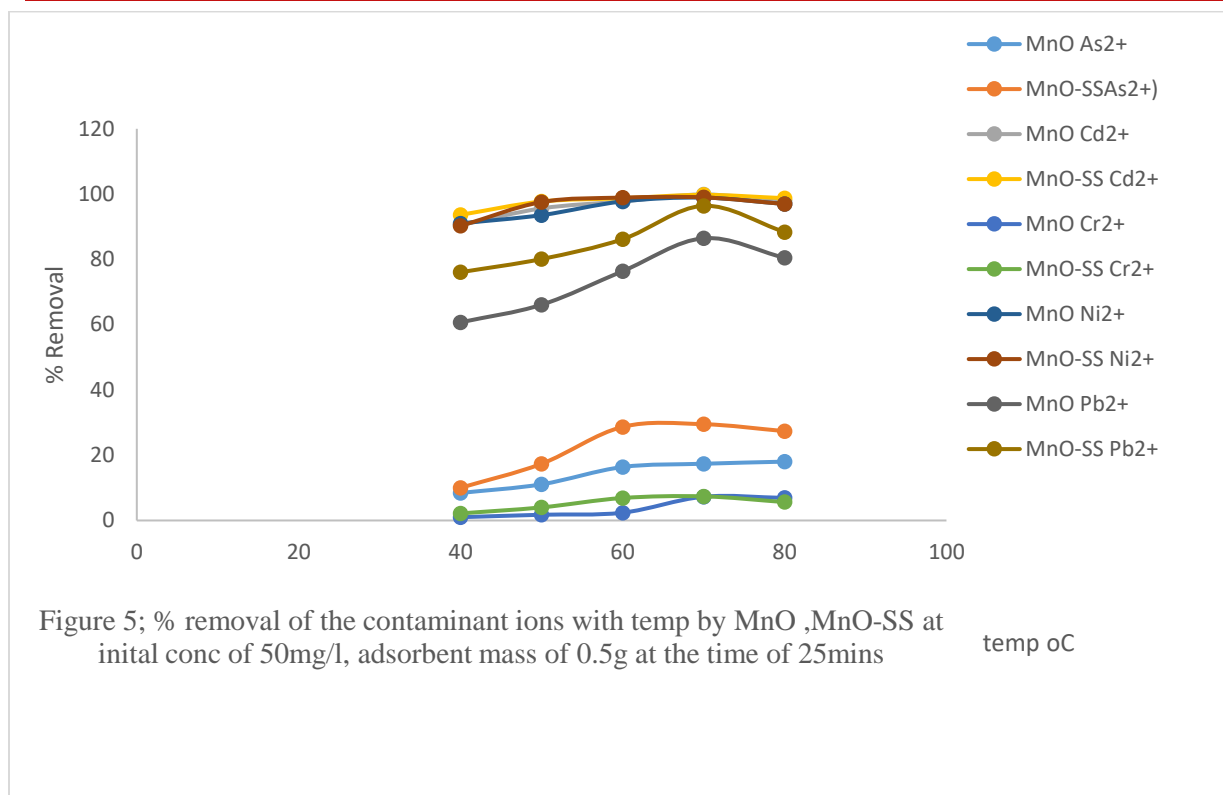
Figure 4: % removal of the contaminant ions with time by MnO, MnO-SS at initial conc. of 50ppm, adsorbent mass of 0.5 and temp. of 40°C

Percentage removal of the contaminant ions responded with increase in time with a slight slow removal efficient towards the end of adsorption period. The rapid initial removal efficiency observed could be attributed to more metal contaminant ions interaction with the uncovered surfaces of the adsorbents as time elapsed (Shi et al., 2013) which resulted to the distributions of  $As^{3+}$ ,  $Cd^{2+}$ ,  $Cr^{6+}$ ,  $Ni^{2+}$  and  $Pb^{2+}$  ions on the surfaces of MnO and MnO-SS Nano materials. The slight decline in % removal could be as a result of Adsorption capacity equilibrium attainment of the adsorbents (Kilic et al., 2011).

The highest adsorption capacities of MnO-SS and MnO Nano materials were observed at the removal processes of  $Ni^{2+}$  and  $Cd^{2+}$  with the maximum % removal of 98.7% and 99.4% (Figure 4.8). The least removal efficiencies of the Nano materials were observed in the processes of  $Cr^{6+}$  and  $As^{3+}$  removal. The maximum % removal values for the two metal ions ( $Cr^{6+}$  and  $As^{3+}$ ) were observed to be at 7.3 and 29.5% respectively and the order of % removal of various contaminant metal ions was observed as;  $Ni^{2+} > Cd^{2+} > Pb^{2+} > As^{3+} > Cr^{6+}$ . Again, affinity of metal ion contaminants to the adsorbents played a huge role on the apparent % removal variations. From the result,  $As^{3+}$  and  $Cr^{6+}$  have lower degree of affinity to the adsorbents than the other metal ions as a substantial amount of  $As^{3+}$  and  $Cr^{6+}$  was not adsorbed on the adsorbent, rather remained in solution.

#### Effects of temperature.

Results of the effects of varying temperature between 40 to 80°C at intervals of 10°C in adsorption processes of metal ion contaminants ( $As^{3+}$ ,  $Cd^{2+}$ ,  $Cr^{6+}$ ,  $Ni^{2+}$  and  $Pb^{2+}$ ) onto ordinary and starch modified metal oxide Nano adsorbent (MnO-SS and MnO) are presented in Figure 5.



Percentage removal of the contaminant metal ions as carried out by MnO; MnO-SS Nano adsorbent and shown on Figure 5. Maximum % removal values for (Ni<sup>2+</sup> and Cd<sup>2+</sup> by MnO; MnO-SS were observed at 93.5%, 96%, and 97%, 98% respectively. Lead ion (Pb<sup>2+</sup>) % removal recorded lower values of 76.4% and 86.2% respectively. Chromium ion (Cr<sup>6+</sup>) has the lowest % removal values of 7.2% and 8% for MnO and MnO-SS Nano materials after arsenic ion (As<sup>3+</sup>) with % removal values of 17.4% and 29.5%.

The study was carried out at initial concentration of 50mg/l, adsorbent mass of 0.5g and time interval of 25 minutes. It was observed from the Figures that % removal seemed to be on the decline as the temperature approached maximum level. The prevailing scenario may be ascribed to breakage of intermolecular bonds between the contaminant ions and the metal oxide of Nano materials at high temperature (Aseel et al., 2014), leading to desorption of adsorbed contaminant ions into the solution. Again, solubility of the metal ion in the solvent at high temperature might result to stronger interaction between the metal ions and solvent than between the metal ions and the adsorbents (MnO-SS and MnO). This scenario may lead to non-availability of the precipitated metal ion contaminant for adsorption (Hanan et al 2010).

#### Effect of initial solution concentration

The initial solution concentration of the solution significantly impacts on the heavy metal removal process. In this study, effects of the initial solution concentration on the adsorption process of various contaminant ions (As<sup>3+</sup>, Cd<sup>2+</sup>, Cr<sup>6+</sup>, Ni<sup>2+</sup> and Pb<sup>2+</sup>) onto adsorbents (MnO-SS and MnO) surfaces by varying the initial concentrations of the ions in the range of 10, 20, 30, 40 and 50ppm, were shown on Figures 6. From Figure 4.14, adsorption of contaminant ions onto MnO-SS and MnO Nano adsorbents reached equilibrium at initial concentrations range of 30 to 40mg/l of the ions. Adsorptions of Pb<sup>2+</sup>, Cd<sup>2+</sup> and Ni<sup>2+</sup> on both MnO and MnO-SS Nano adsorbents experienced



equilibrium at 30mg/l concentrations of the ions. Adsorption surfaces of the MnO and MnO-SS Nano adsorbents got to saturation at the initial concentrations of 40mg/l of  $\text{As}^{3+}$  and  $\text{Cr}^{6+}$ . The trend of % removal of the metal ion contaminants by MnO and MnO-SS Nano adsorbents is shown in this order;  $\text{Ni}^{2+} > \text{Pb}^{2+} > \text{Cd}^{2+} > \text{As}^{3+}$ .

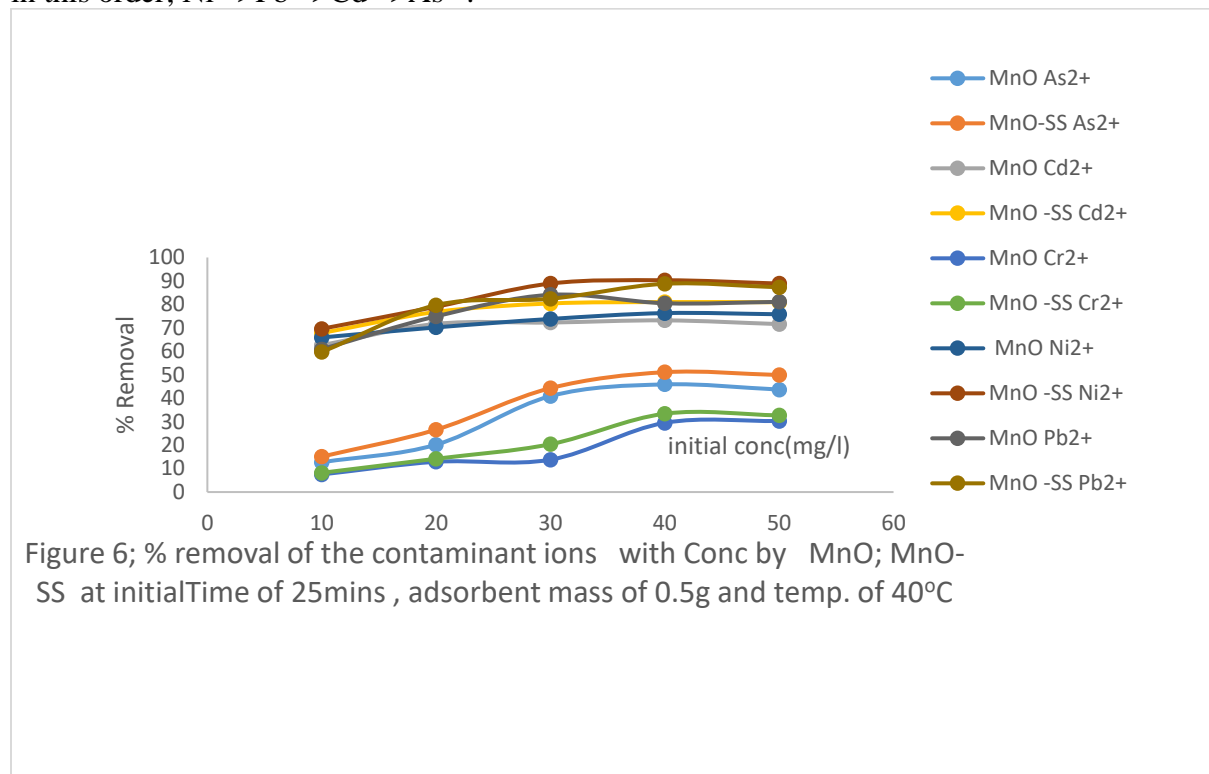


Figure 6; % removal of the contaminant ions with Conc by MnO; MnO-SS at initialTime of 25mins , adsorbent mass of 0.5g and temp. of 40°C

From the Figure, % removal of contaminant ions progressed as the initial concentrations of various ions ( $\text{As}^{3+}$ ,  $\text{Cd}^{2+}$ ,  $\text{Cr}^{6+}$ ,  $\text{Ni}^{2+}$  and  $\text{Pb}^{2+}$ ) increased until adsorption process got to equilibrium point (which is depicted as a plateau in the curves) where percentage removal began to decline. The reason could be attributed to non-availability of active sites occasioned by the saturation of adsorbent surfaces as also observed by (Cabrera et al., 2005, Sobhy, 2014, Uzoije et al., 2015). Several studies have reported that an increase in the initial concentration resulted in an improvement in the adsorption capacity at the initial stage and a decrease in the overall heavy metal removal efficiency due to non-availability of active sites. (Coruh & Ergun, 2009; Cabrera et al., 2005; Peric et al., 2004; Erdem et al., 2004; Oren & Kaya, 2006; Akgu et al., 2006).

### Effects of adsorbent dosage

Effects of adsorbent dosage was investigated by varying adsorbent mass of MnO and MnO-SS from 0.1 to 0,5g under the contaminant ion initial concentration of 50mg/l, time interval of 25mins and temperature value of 40°C and were represented in Figures 7.

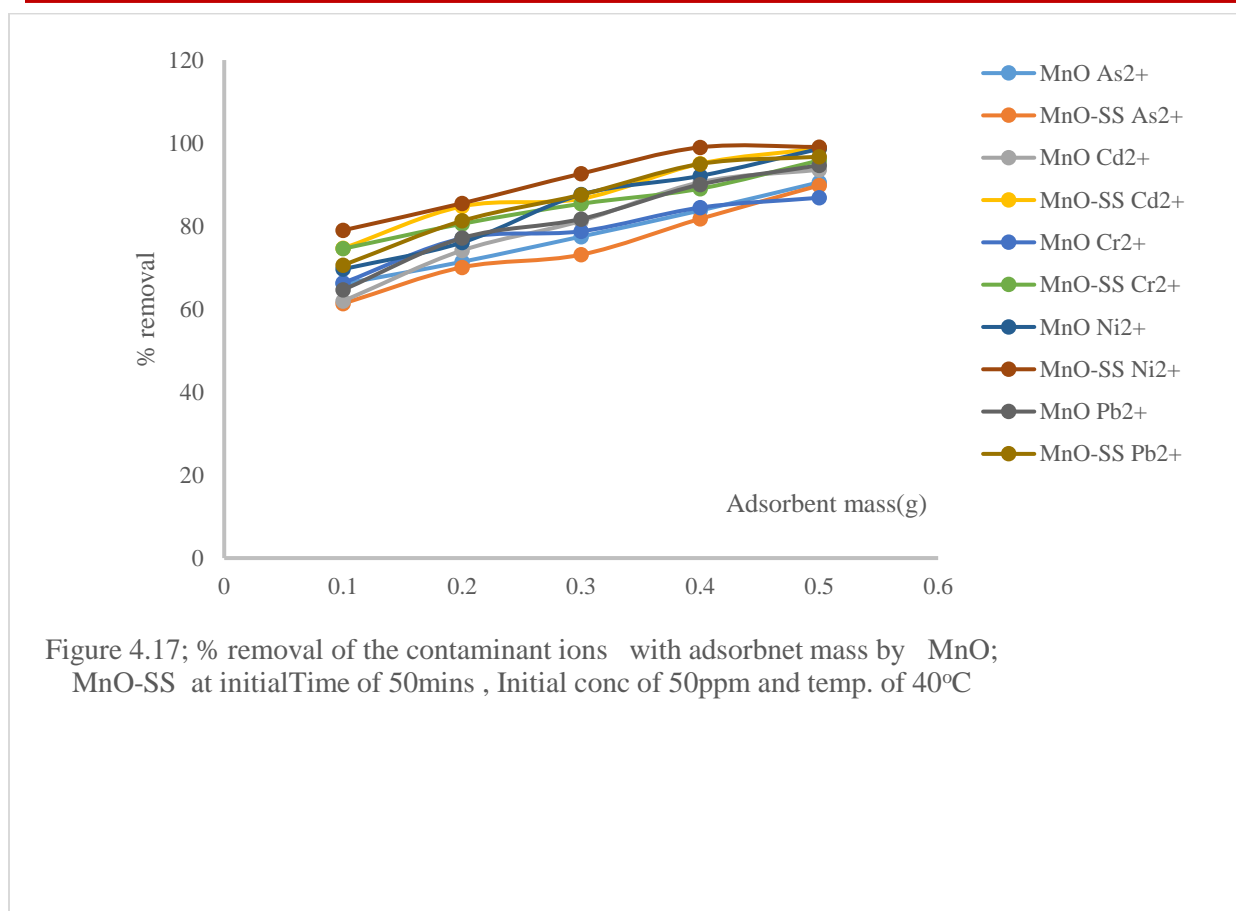


Figure 4.17; % removal of the contaminant ions with adsorbent mass by MnO; MnO-SS at initialTime of 50mins , Initial conc of 50ppm and temp. of 40°C

There was rapid increase in % removal of metal ion contaminants ( $\text{As}^{3+}$ ,  $\text{Pb}^{2+}$ ,  $\text{Ni}^{2+}$ ,  $\text{Cd}^{2+}$ ,  $\text{Cr}^{6+}$ ) with increase in adsorbent dosage from 0.1 to 0.5g. The initial rapid % Removal increase lasted to a point where the onward increase became slower (Zahoora *et al.*, 2019, Nagendran & Noor, 2015, Sohby 2014) attributed the % removal pattern to availability of greater number of adsorbing sites and the apparent slow removal process to saturation of the adsorbent sites. This scenario was observed in all the Nano adsorbents. However, the slowing down of % removal was observed at adsorbent dosage mass of between 0.4 and 0.5g for MnO and MnO-SS suggesting that MnO and MnO-SS have more readily available adsorption sites for the uptake of the metal contaminant ions.

### Conclusion

Adsorption processes of  $\text{As}^{3+}$ ,  $\text{Cd}^{2+}$ ,  $\text{Cr}^{6+}$ ,  $\text{Ni}^{2+}$  and  $\text{Pb}^{2+}$  contaminant ions through column experiment in which the Nano materials prepared from ordinary (MnO) and starch modified (MnO-SS) metal oxides as adsorbents have been evaluated. In adsorbent characterization, XRD results confirmed larger particle sizes for the starch modified Nano adsorbents of MnO than the ordinary Nano adsorbents. It is recommended based upon the results obtained that starch should be incorporated in the synthesis of the metal oxide MnO used as adsorbent since it improves the surface area and enhances greater adsorption.

## References

- Akgu, M., Karabakan, A., Acar, O. & Yurum, Y. (2006). Removal of silver (I) from aqueous solutions with clinoptilolite. *Microporous and Mesoporous Materials*, 94, 99–104.
- Aseel M. Aljeboree, Abbas N. Alshirifi, & Ayad F. (2014). Kinetics and equilibrium study for the adsorption of textile dyes on coconut shell activated carbon; *Arabian Journal of Chemistry* 43. 124-132
- Cabrera, C., Gabaldon, C. & Marzal, P. (2005). Sorption characteristics of heavy metal ions by a natural zeolite. *Journal of Chemical Technology and Biotechnology*, 80, 477-481
- Chen, Y., Pan, B., Li, H., Zhang, W., Lv, L. & Wu, L. (2010). Selective removal of Cu (II) ions by using cation-exchange resin-supported polyethyleneimine (PEI) nanoclusters. *Environmental Science and Technology*, 44: 3508-3513.
- Coruh, S. & Ergun, O.N. (2009). Ni<sup>2+</sup> removal from aqueous solutions using conditioned clinoptilolites: kinetic and isotherm studies. *Environmental Progress & Sustainable Energy*, 28, 162–172.
- Das, N. (2015). Recovery of precious metals through biosorption—a review. *Hydrometallurgy*, 103(1), 180-189.
- El-Sherif, I. Y., Tolani, S., Oforu, K., Mohamed, O. A. & Wanekaya, A. K. (2013). Polymeric nanofibers for the removal of Cr (III) from tannery waste water. *Journal of Environment 'al Management*, 129, 410–413.
- Erdem, E., Karapinar, N. & Donat, R. (2004). The removal of heavy metal cations by natural zeolites. *Journal of colloidal and Interface Science*, 280(2), 309 – 314.
- García-Niño, W. R., & Pedraza-Chaverri, J. (2014). Protective effect of curcumin against heavy metals-induced liver damage. *Food Chemistry and Toxicology*, 69, 182–201.
- Hanan E. Osman, Reham K. Badwy, & Hanan F. A., (2010). Usage of some agricultural by-products in the removal of some heavy metals from industrial wastewater. *Journal of Phytology*, 2(3): 51–62
- Ho, Y.S. & McKay, G. (1999). The sorption of Lead (II) on peat. *Water Research*, 33, 578-584.
- Isidorov, V. (1997). Introduction to Chemical Eco-toxicology. Saint-Petersburg State University, 54-58.
- Kilic, M., Apaydin-Varol, E., & Putun, E.A., (2011). Adsorptive removal of phenol from aqueous solutions on activated carbon prepared from tobacco residues: Equilibrium, kinetics and thermodynamics. *Journal of Hazardous Materials*, 189, 397–403.
- ‘Konne, J. L., & Opara, K. (2014). Remediation of nickel from crude oil obtained from Bomu Oil Field using cassava waste water starch stabilized magnetic nanoparticles. *Energy and Environmental Research*, 4(1), 25-31.
- Langergren, S., & Svenska, B. K. (1898); Zur theorie der sogenannten adsorption gelöster stoffe. *Veternskapsakad Nandlingar*, 24, 1-39.
- Nagendran S. & Noor S. S. (2015). Dye adsorbent by pineapple activated carbon: H<sub>3</sub>PO<sub>4</sub> and NaOH Activation ;arpn *Journal of Engineering and Applied sciences*. 10(20), november, issn 1819-6608
- Oren, A.H. & Kaya, A. (2006) Factors affecting adsorption characteristics of Zn<sup>2+</sup> on two natural zeolites. *Journal of Hazardous Materials*, 13, 59–65.
- Peric, J., Trgo, M. & Medvidovic, N.V. (2004). Removal of zinc, copper and lead by natural zeolite-a comparison of adsorption isotherms. *Water Research*, 38, 1893-1899.

- Qasem, N. A. A., Mohammed, R. H., & Lawal, D.U. (2021). Removal of heavy metal ions from wastewater: a comprehensive and critical review. *npj Clean Water*, 4, 36; <https://doi.org/10.1038/s41545-021-00127-0>
- Qu, X., P., Alvarez, P. J. J., & Li, Q. (2013). Applications of nanotechnology in water and wastewater treatment. *Water Research*, 47: 3931–3946.
- Shi, Y., Kong, X., Zhang, C., Chen, Y., & Hua, Y., (2013). Adsorption of soy isoflavones by activated carbon: kinetics, thermodynamics and influence of soy oligosaccharides. *Chemical Engineering Journal*, 215–216, 113–121.
- Sikder M.T., Mihara Y., Islam M.S., Saito T., Tanaka S., & Kurasaki M., (2014). Preparation and characterization of chitosan-carboxymethyl- $\beta$ -cyclodextrin entrapped nanozero-valent iron composite for Cu (II) and Cr (IV) removal from wastewater. *Chemical Engineering Journal*, 236: 378-387.
- Sobhy, M (2014), Yakout Removal of the hazardous, volatile, and organic compound benzene from aqueous solution using phosphoric acid activated carbon from rice husk Yakout. *Chemistry Central Journal* 8(52), 2 of 7
- Taseidifar, M., Makavipour, F., Pashley, R. M. & Rahman, A. F. M. M. (2017). Removal of heavy metal ions from water using ion flotation. *Environmental Technology and Innovations*, 8, 182–190.
- Teh, C. Y., Wu, T. Y. & Juan, J. C. (2014). Potential use of rice starch in coagulation-flocculation process of Agro-industrial wastewater: Treatment performance and flocs characterization. *Ecology and Engineering*, 71: 509–519.
- Uzoije, A. P., Pascal A. P, Njoku1 C., Atu Ayuk1 A., Justus I. & Okolie1 (2015). Equilibrium, Thermodynamic and Kinetic Studies on Adsorption of Zinc (II) From Solutions Using Different Low-Cost Adsorbents. *American Journal of Chemistry and Applications*, 2(6): 129-140
- Wang, J. & Chen, C. (2009). Biosorbents for heavy metals removal and their future. *Biotechnology Advances*, 195–226.
- Zahoor, M., Ullaha, A & Alam, S. (2019). Removal of Enrofloxacin from Water through Magnetic Nanocomposites Prepared from Pineapple Waste Biomass Surface. *Engineering and Applied Electrochemistry*, 55(5), 536–547.